

The SRTM Mission: A World-Wide 30 m Resolution DEM from SAR Interferometry in 11 Days

RICHARD BAMLER, Wessling

ABSTRACT

The Shuttle Radar Topography Mission (SRTM) to be launched in September 1999 will use C-band and X-band interferometric synthetic aperture radars (InSAR) to acquire the most complete homogeneous 30 m resolution Digital Elevation Model (DEM) of the world up to date. 80% of the Earth's land mass (i.e. between 60°N and 56°S) will be mapped during an 11-day Space Shuttle mission. The digital topographic map products will meet the Interferometric Terrain Height Data (ITHD)-2 specifications: 30 m x 30 m spatial sampling with 16 m absolute vertical height accuracy, 10 m relative vertical height accuracy and 20 meter absolute horizontal accuracy. The paper gives a brief overview of the SRTM system and products.

1. INTRODUCTION

Synthetic Aperture Radar (SAR)

For the purpose of this paper it is sufficient to understand that a - spaceborne or airborne - SAR images the Earth's surface in a side-looking fashion as depicted in figure 1. While the sensor is moving along its path/orbit it transmits microwave pulses to the ground and receives the echoes of each pulse scattered back from the Earth surface. The SAR receiver detects the stream of echoes coherently, i.e. with respect to their amplitude and phase. This allows the formation of a synthetic aperture in a subsequent signal processing step. The result is a high resolution image of the microwave reflectivity of the ground. Typical spatial resolutions of spaceborne SAR's are 5 m - 100 m. In the following we will refer to microwave pulses of wavelength $\lambda = 3$ cm (X-band) or $\lambda = 5.6$ cm (C-band).

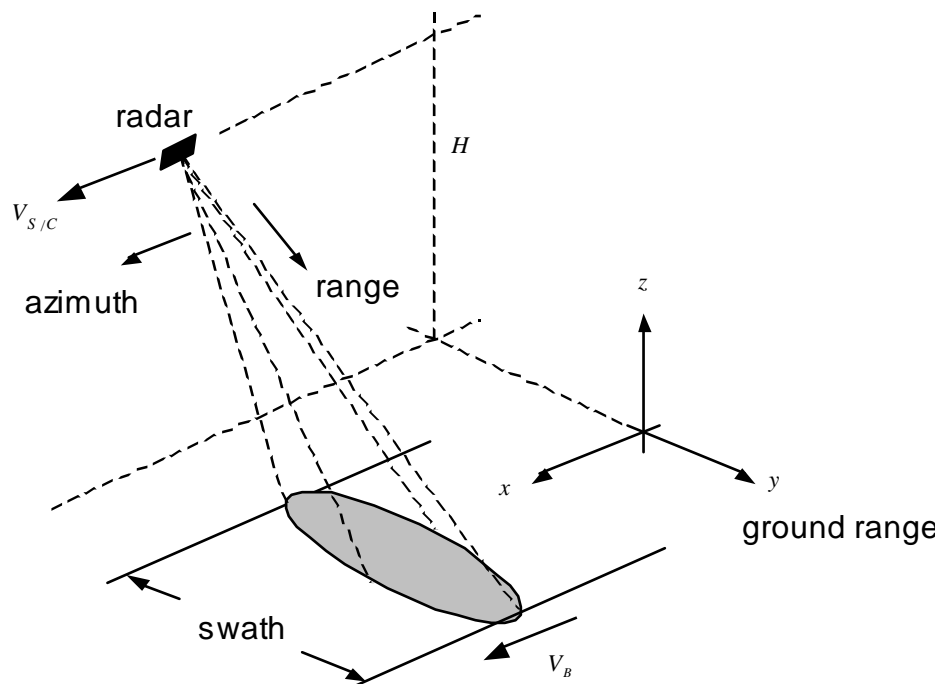


Figure 1: SAR imaging geometry.

Since both the radar hardware and the processing are coherent such that they preserve the phase information, each SAR image pixel is a complex number. Its amplitude is a measure for microwave reflectivity and its phase reflects the distance (range R) of the respective ground resolution cell to the SAR antenna. A variation of range as small as $\lambda/2$ results in a full cycle phase shift of 2π .

Interferometric SAR (InSAR)

The high sensitivity of the SAR pixel phase to range is exploited in InSAR. Two SAR's are used to image the same ground area from two (almost) parallel orbits (figure 2). A typical spatial separation (baseline) of the orbits is in the order of 10 m – 500 m. In the case of *repeat-pass* InSAR the two SAR images are taken at different times (e.g. several days apart) possibly by the same radar. *Single-pass* interferometry, on the other hand, requires a dual channel radar system with a transmit/receive master antenna and a receive-only slave antenna. In either case the two SAR's or channels measure slightly different ranges R_1 and R_2 for any ground point. Hence, the corresponding image pixels, although equally 'bright', exhibit different phase. The phase *difference* (or: *interferometric phase*) ϕ of two corresponding pixels is related to the range difference (parallax) via

$$\phi = p \frac{2\pi}{\lambda} (R_2 - R_1)$$

where $p = 2$ for repeat-pass and $p = 1$ for single-pass interferometry, respectively. This phase is measured pixel-wise by (i) co-registration of the two SAR images to within a small fraction of a pixel and (ii) complex conjugate multiply of the registered images. Every pixel of the resulting interferogram carries phase, i.e. parallax, information – even in areas of low or zero contrast. From this two-dimensional phase field the DEM of the imaged area can be computed after the 2π -ambiguity of the phase measurement has been removed by a procedure called *phase unwrapping*.

Figure 3 shows an example of DEM formation from InSAR data. For more detailed information on InSAR see, e.g., (Bamler and Hartl 1998; Gabriel and Goldstein 1988; Gatelli et al. 1994; Graham 1974; Massonnet and Rabaute 1993; Prati and Rocca 1990; Rodriguez and Martin 1992; Zebker and Goldstein 1986).

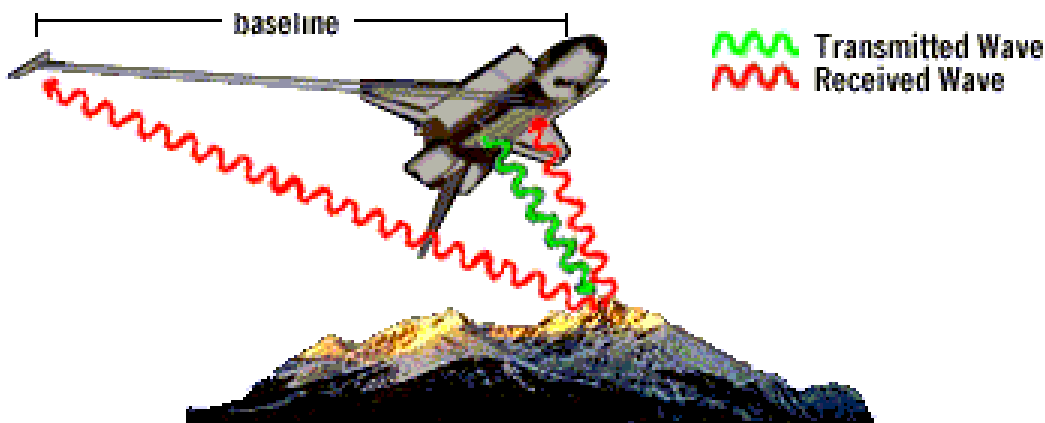


Figure 2: SRTM single-pass InSAR configuration (not in scale: baseline exaggerated).

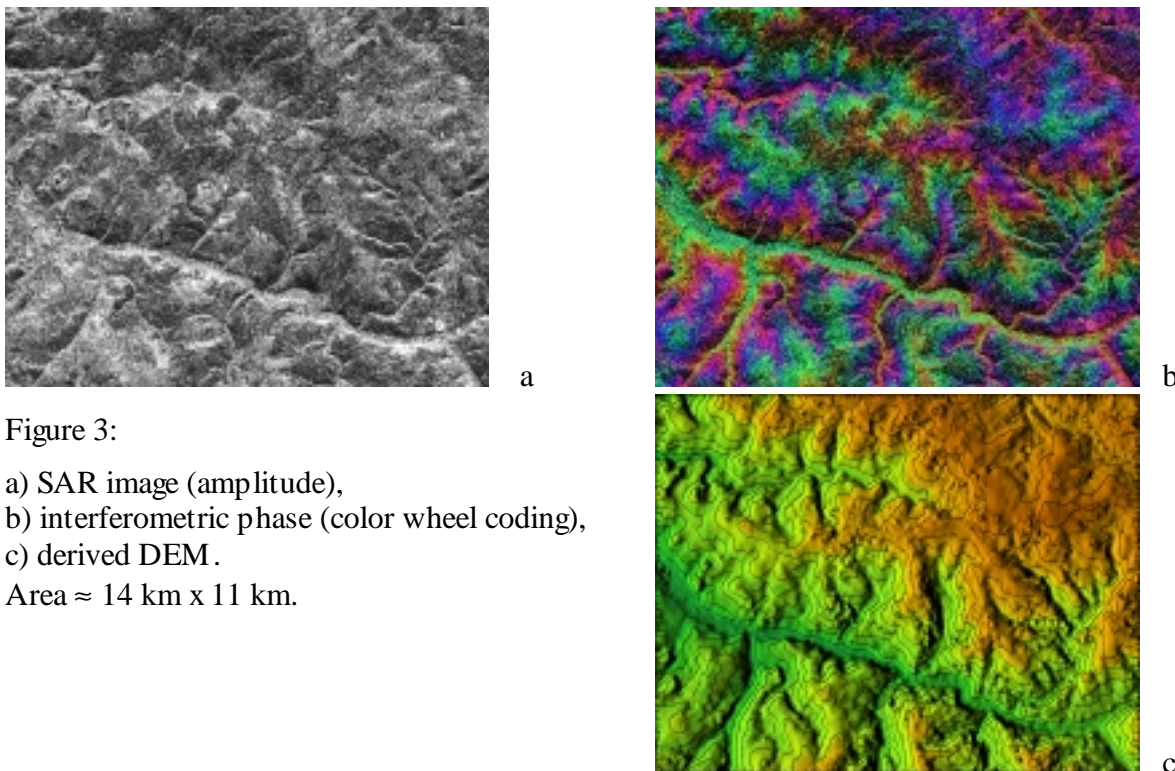


Figure 3:

- a) SAR image (amplitude),
 - b) interferometric phase (color wheel coding),
 - c) derived DEM.
- Area \approx 14 km x 11 km.

Height Errors and Phase Errors

Height errors in the final interferometric DEM may have different sources:

- Any error in the *attitude* (roll) of the interferometric baseline will result in a tilt of the DEM by the same angle (cf. figure 2). An error in the *baseline length* give rise to under/overestimation of height and to a small nonlinear distortion of the DEM. Both these errors are of large spatial scale and can be reduced by exploiting ground control points.
- *Atmospheric inhomogeneities* may cause spatially varying wave propagation delays. Typical spatial scales are in the km regime (Dupont 1996; Goldstein 1995; Hanssen 1999; Massonnet et al. 1995). For single-pass configurations these signal delays cancel out, since due to the small interferometric baseline both antennas ‘look’ through the same atmospheric condition. In repeat-pass interferograms, however, atmospheric inhomogeneities cause phase errors mostly in the order of a fraction of a phase cycle. Optimum averaging of several repeat-pass interferograms is often applied to reduce this effect (Ferretti et al. 1997).
- *Phase measurement noise* translates into random height errors of short correlation length via

$$\delta_h = \frac{\lambda R \sin \theta}{p 2 \pi B_{\perp}} \delta_{\phi}$$

where B_{\perp} is the baseline component perpendicular to the radar look direction. With single-pass interferometers phase noise is caused by thermal and quantization noise of the radar receivers. Repeat-pass systems, on the other hand, suffer from temporal decorrelation of the imaged scatterers: if the scattering properties and/or the locations of the subscatterers in a resolution element have changed between the two acquisitions, the phase information deteriorates and phase noise is experienced (Zebker and Villasenor 1992). This effect reduces e.g. the DEM accuracy over forest areas at short wavelengths and makes the acquisition of DEM’s over water bodies impossible by repeat-pass interferometry. Hence, for high precision DEM generation a single-pass interferometer is preferred to a repeat-pass system.

High frequency noise-induced errors determine what is often referred to as *relative accuracy*, while *absolute accuracy* also includes large scale (attitude-induced) errors.

2. THE SHUTTLE RADAR TOPOGRAPHY MISSION (SRTM)

Two successful Shuttle Radar Lab (SRL) missions of the SIR-C/X-SAR instrument were flown in 1994. The radar hardware consisted of the US fully polarimetric L- and C-band SAR's and a German/Italian X-band SAR. During the second flight interferometric data were collected in the repeat-pass mode and in all wavelengths and polarizations. Sample data have been processed to topographic maps to prove the feasibility of interferometry with SIR-C/X-SAR and its platform, the space shuttle.

SRTM reuses the SIR-C/X-SAR hardware augmented by secondary C- and X-band receive (slave) antennas mounted at the tip of a 60 m boom extending from the shuttle's cargo bay (figure 4) to form a single-pass interferometer (Bamler et al. 1996; Jordan et al. 1996).

The SRTM is a cooperative effort between NASA, the US National Imagery and Mapping Agency (NIMA), the Italian Space Agency (ASI), and the German Aerospace Center (DLR). Citing the official SRTM WWW home page (JPL 1999) the *mission objective* is as follows:

- “To use C-band and X-band interferometric synthetic aperture radars (...) to acquire topographic data over 80% of Earth's land mass (between 60°N and 56°S) during an 11-day Shuttle mission.
- Produce digital topographic map products which meet Interferometric Terrain Height Data (ITHD)-2 specifications (30 meter x 30 meter spatial sampling with 16 meter absolute vertical height accuracy, 10 meter relative vertical height accuracy and 20 meter absolute horizontal circular accuracy). All accuracies are quoted at the 90% level, consistent with National Mapping Accuracy Standards.”

The mission features several ‘firsts’:

- First single-pass spaceborne InSAR system
- First simultaneous dual-polarization wide-swath ScanSAR dual frequency (C-band and X-band) interferometric SAR
- Largest rigid structure (60 m boom) ever flown in space

Tables 1 summarizes some characteristics of the mission.

Launch / Landing	September 16 / 27, 1999
Mission Duration	11 Days
Project Start / End	August 1996 / March 2001
Project Life Cycle	54 months (36 months start to launch; 18 months data processing)
Total Cost	\$ 220M (\$120M US; \$50M DLR; \$50M KSC)
Payload Weight	ca.13,600 kg (ca.15 mid-sized cars)
Energy Usage	ca.900 kWh (enough to power a typical home for 2-3 months)
Orbit Altitude	233 km
Orbit Inclination	57°
Planned Data Takes	ca.1,000 (over 80% of Earth's land mass)
Data Acquisition	> 80 hours
Data Recording Rate	180 Mbits/sec for C-band, 90 Mbits/sec for X-band
Total Raw Radar Data	ca. 9.8 Terabytes (15,000 CDs)
Data Tapes	ca. 300 high density tapes

Table 1: SRTM Mission Characteristics.

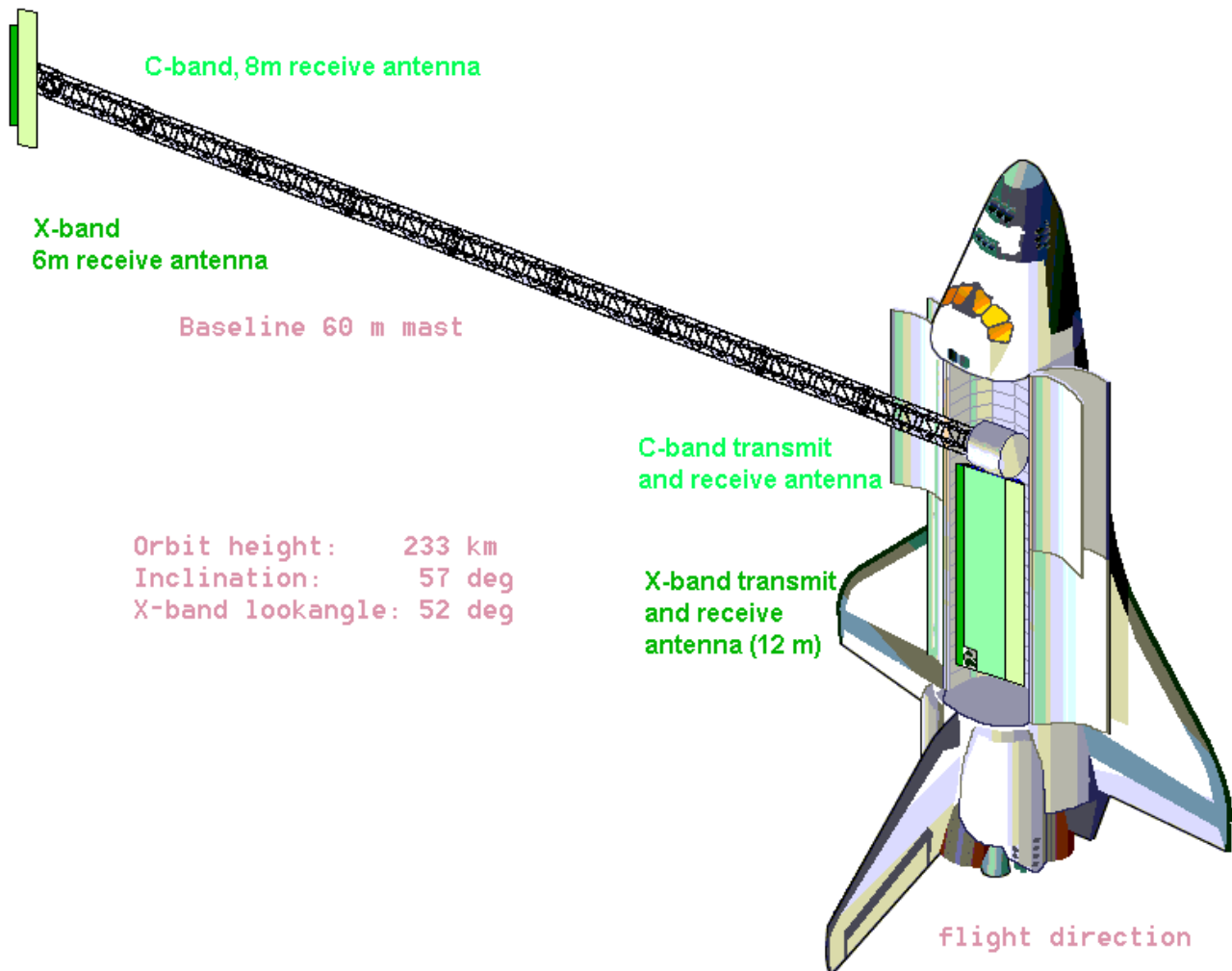


Figure 4 : The SRTM interferometer with deployed 60 m boom.

SRTM Mapping Modes and Coverage

In order to achieve global coverage a swath width of ca. 220 km is required. Therefore the C-band interferometer must be operated in the so-called ScanSAR mode. In this mode the antenna beam is electronically steered towards different elevation angles in a repeated stepwise fashion. Thus, four narrow but overlapping subswaths are imaged quasi simultaneously to form the 225 km wide swath. By exploiting the polarimetric capability of the C-band system two subswaths will be illuminated at a time using orthogonal polarizations. Hence, a ScanSAR duty cycle of 1:2 rather than 1:4 is achieved for each subswath. ScanSAR interferometry requires different processing algorithms. For ScanSAR processing and ScanSAR interferometry see, e.g. (Bamler and Eineder 1996; Bamler et al. 1999, Monti Guarnieri and Prati 1996; Monti Guarnieri et al. 1994; Moore et al. 1981; Moreira et al. 1996; Tomiyasu 1981).

The X-band antenna cannot be steered electronically. It will be operated at a fixed off-nadir look angle of 52° and a swath width of about 45 km. Due to the shorter wavelength and the non-ScanSAR mode the X-band interferograms will give higher relative height accuracy by almost a factor of 2. The penalty is that X-band data will not give full coverage. Figures 5 and 6 show the coverage for C- and X-band data, respectively.

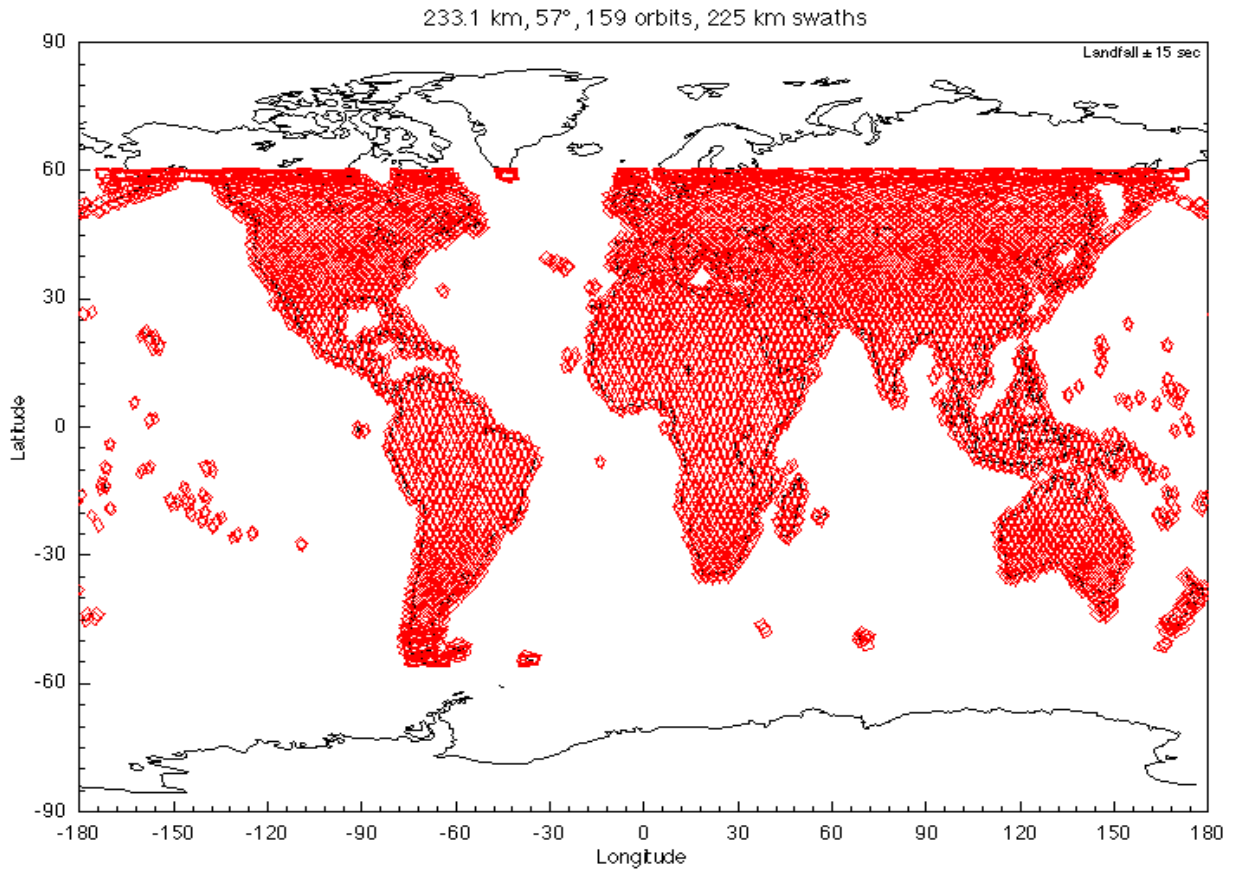


Figure 5: Coverage of SRTM using ascending and descending passes. The C-band system covers the red areas without gaps, the X-band radar has narrower swath (see figure 6).

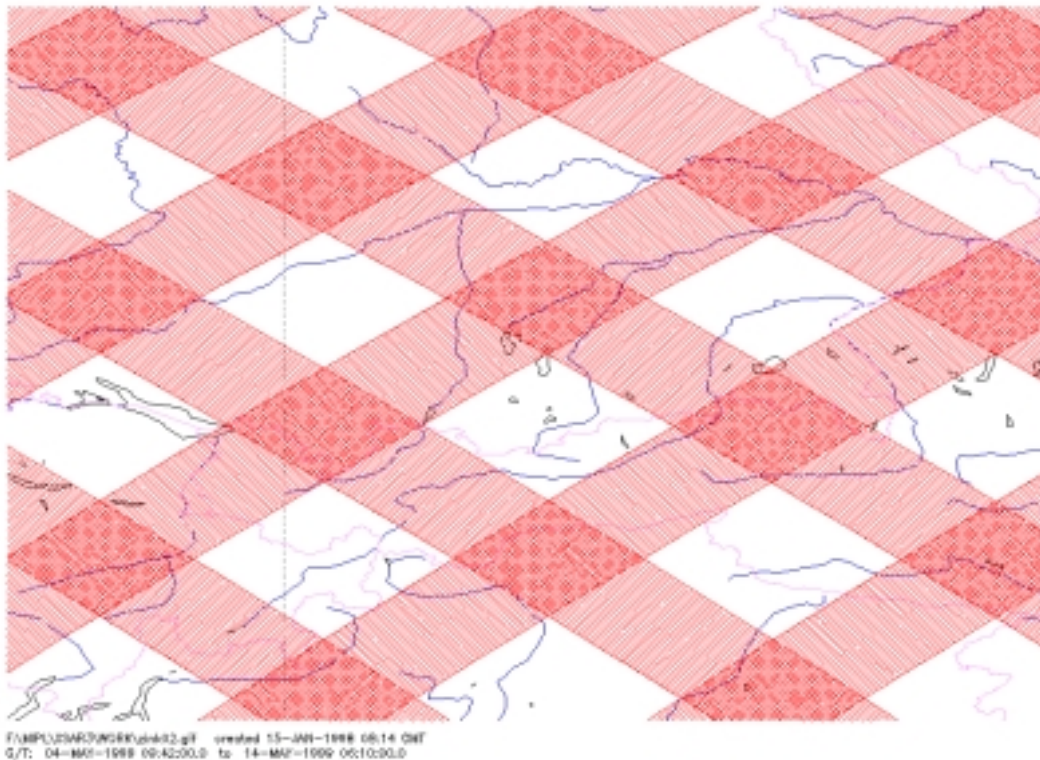


Figure 6: Detailed view of SRTM X-band data coverage (Bavaria/Germany). Swath width ≈ 45 km.

SRTM Products

DLR has developed an operational processing system for the X-band SRTM data consisting of the SAR processor *BSAR* (Breit et al. 1997), the Generic System for InSAR processing *GENESIS* (Eineder and Adam 1997) and the DEM generation and mosaicking system *GeMoS* (Roth et al. 1998). This processing chain is also used for DEM generation from ERS-1/2 tandem or Radarsat data. An example of a DEM mosaic produced at DLR is shown in figure 7. The SRTM C-band data processor has been developed by JPL/Pasadena and will be operated by NIMA.

The primary SRTM data products will be:

- X-band ITED-2 DEM's: 1 arcsec Interferometric Terrain Elevation Data (table 2);
- C-band ITED-2 DEM's: 1 arcsec Interferometric Terrain Elevation Data (table 3);
- C-band ITED-1 DEM's: 3 arcsec Interferometric Terrain Elevation Data (table 3);

All X-band SRTM data will be processed and distributed by DLR, except for data over Italian territory, which will be provided by ASI. The X-band ITED-Level 2 data will be available starting in mid 2000, the C-band ITED-Level-1 and -2 data should be ready for release by mid 2001. The progress of data processing can be monitored by users via Internet. All X-band SRTM data will be catalogued and made available to users.

The C-band ITED-2 data will be available for the national territory of Germany, the USA and to-be-determined areas for jointly agreed scientific investigations subject to NASA-NIMA data-use-guidelines. C-band ITED-1 products will be available globally. X-SAR elevation products will be available globally.

Accuracy Specifications	
Absolute Horizontal Accuracy	90% Circular Error< 20 meters
Relative Horizontal Accuracy	90% Circular Error< 15 meters
Absolute Vertical Accuracy	90% Linear Error< 16 meters
Relative Vertical Accuracy	90% Linear Error< 6 meters
Spatial Resolution	30 m x 30 m
Horizontal Datum	WGS 84
Vertical Datum	WGS 84 ellipsoid
Product Format	
Block Definition	fixed, 15' raster in lat and long
Reference Origin	Southwest corner
Data Record Sequence	Ascending (west to east) longitude
Data Value Sequence	Ascending (south to north) latitude
Posting	<u>Latitude</u> <u>Longitude</u>
0 ⁰ - 50 ⁰ N - S	1 arcsec 1 arcsec
50 ⁰ - 60 ⁰ N - S	1 arcsec 2 arcsec
Data Format Representation	16-bit signed integer
Physical Units	meters
Medium of Distribution	CD-ROM /INTERNET

Table 2: SRTM X-Band Level-2 Terrain Height Maps.

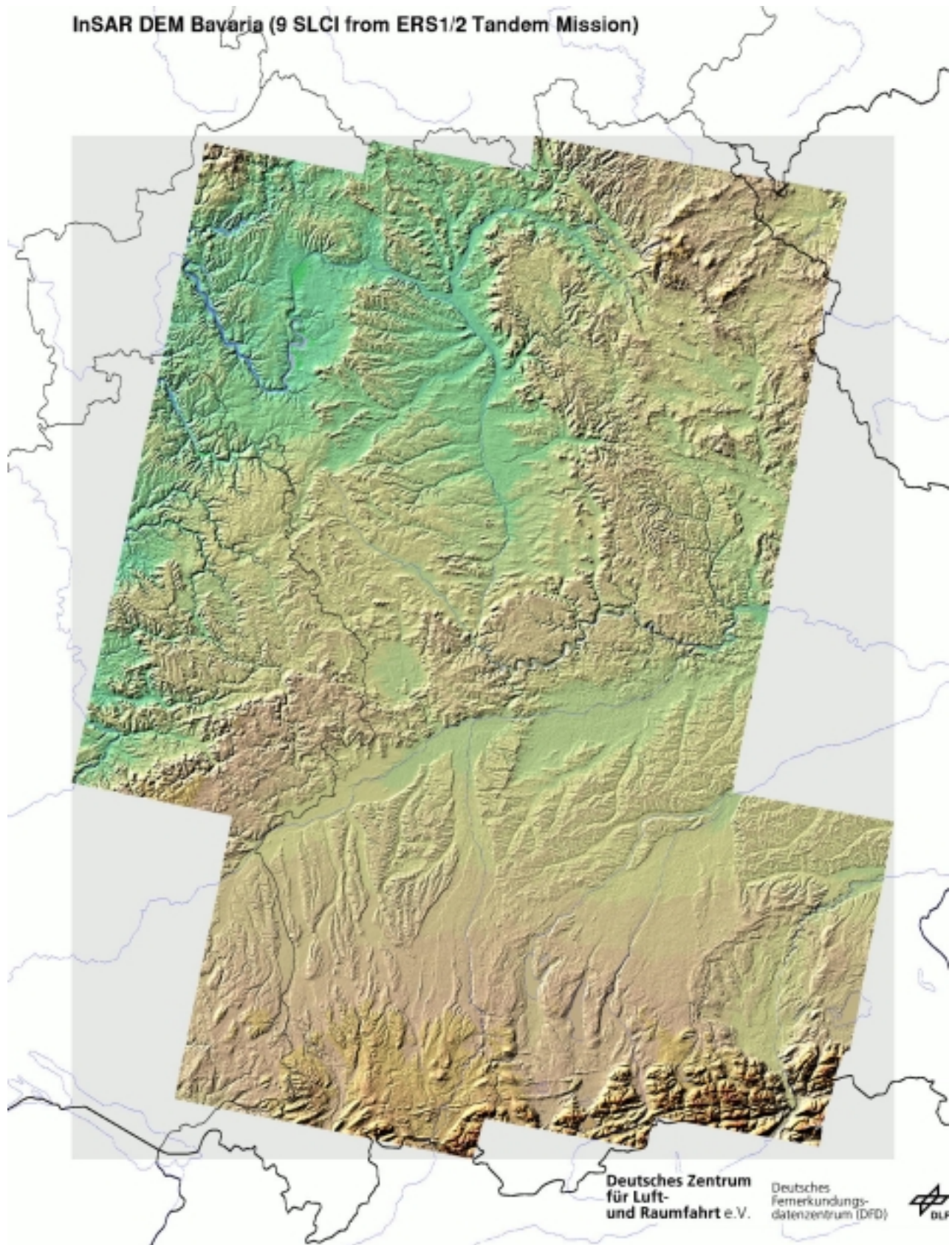


Figure 7: DEM of Bavaria/Germany produced from 9 ERS-1/2 tandem data set pairs.
Size \approx 300 km x 200 km.

	Level-1 Terrain Height Maps	Level-2 Terrain Height Maps
Accuracy Specifications		
Abs. Horizontal Accuracy	90% Circular Error< 20 meters	90% Circular Error< 20 meters
Rel. Horizontal Accuracy	90% Circular Error< 15 meters	90% Circular Error< 15 meters
Abs. Vertical Accuracy	90% Linear Error< 16 meters	90% Linear Error< 16 meters
Rel. Vertical Accuracy	90% Linear Error< 10 meters	90% Linear Error< 10 meters
Spatial Resolution	30 m x 30 m	30 m x 30 m
Horizontal Datum	WGS 84	WGS 84
Vertical Datum	WGS 84 ellipsoid	WGS 84 ellipsoid
Product Format		
Block Definition	fixed, 15' raster in lat and long	fixed, 15' raster in lat and long
Reference Origin	Southwest corner	Southwest corner
Data Record Sequence	Ascending (west to east) long	Ascending (west to east) long
Data Value Sequence	Ascending (south to north) lat	Ascending (south to north) lat
Posting	<u>Latitude</u> <u>Longitude</u>	<u>Latitude</u> <u>Longitude</u>
0 ⁰ - 50 ⁰ N - S	3 arcsec 3 arcsec	1 arcsec 1 arcsec
50 ⁰ - 60 ⁰ N - S	3 arcsec 6 arcsec	1 arcsec 2 arcsec
Data Format Representation	16-bit signed integer	16-bit signed integer
Physical Units	meters	meters
Medium of Distribution	CD-ROM /INTERNET	CD-ROM / INTERNET

Table 3: SRTM C-Band Terrain Height Maps.

3. ACKNOWLEDGEMENTS

The author would like to thank M. Werner, H. Runge, N. Adam, W. Knöpfle and A. Roth of DLR's SRTM team as well as JPL for providing material for this paper.

4. REFERENCES

Bamler, R. and M. Eineder (1996): "ScanSAR processing using standard high precision SAR algorithms." *IEEE Transactions on Geoscience and Remote Sensing*, 34(1), pp. 212-218.

Bamler, R., Eineder, M. and H. Breit (1996): "The X-SAR single-pass interferometer on SRTM: Expected performance and processing concept." *EUSAR'96*, Königswinter, Germany, pp.181-184.

Bamler, R. and P. Hartl (1998): "Synthetic aperture radar interferometry." *Inverse Problems*, 14, R1-R54.

Bamler, R., Geudtner, D., Schättler, B., Vachon, P. W., Steinbrecher, U., Holzner, J., Mittermayer, J., Breit, H. and A. Moreira (1999): RADARSAT ScanSAR interferometry, *International Geoscience and Remote Sensing Symposium IGARSS'99*.

Breit, H., Schättler, B. and U. Steinbrecher (1997): "A high precision workstation-based chirp scaling SAR processor." *International Geoscience and Remote Sensing Symposium IGARSS'97*, pp. 465-467.

Dupont, S. (1996): "Atmospheric artifacts in SAR interferometry." *3rd ERS Symposium*, Florence, Italy, <http://florence97.ERS-symposium.org/>.

Eineder, M. and N. Adam (1997): "A flexible system for the generation of interferometric SAR products." *International Geoscience and Remote Sensing Symposium IGARSS'97*, Singapore, pp. 1341-1343.

- Ferretti, A., Prati, C., Rocca, F. and A. Monti Guarnieri (1997): "Multibaseline SAR interferometry for automatic DEM reconstruction." *3rd ERS Workshop*, Florence, Italy, <http://florence97.ERS-symposium.org/>.
- Gabriel, A. K. and R. M. Goldstein (1988): "Crossed orbit interferometry: theory and experimental results from SIR-B." *International Journal of Remote Sensing*, 9(5), pp. 857-872.
- Gatelli, F., Monti Guarnieri, A., Parizzi, F., Pasquali, P., Prati, C. and F. Rocca (1994): "The wavenumber shift in SAR interferometry." *IEEE Transactions on Geoscience and Remote Sensing*, 32(4), pp. 855-865.
- Goldstein, R. (1995): "Atmospheric limitations to repeat-track radar interferometry." *Journal of Geophysical Research*, 22, pp. 2517-2520.
- Graham, L. C. (1974): "Synthetic interferometer radar for topographic mapping." *Proceedings of the IEEE*, 62(6), pp. 763-768.
- Hanssen, R. (1999): "High-resolution water vapor mapping from interferometric radar measurements." *Science*, 238(5406), pp. 1297-1298.
- Jordan, R. L., Caro, E. R., Kim, Y., Kobrik, M., Shen, Y., Stuhr, F. V. and M. U. Werner (1996): "Shuttle radar topography mapper (SRTM)." *Microwave sensing and synthetic aperture radar*, G. Franceschetti, C. J. Oliver, F. S. Rubertone, and S. Tajbakhsh, eds., SPIE, Bellingham, pp. 412-422.
- JPL. (1999): "SRTM Home Page." <http://www-radar.jpl.nasa.gov/srtm/>.
- Massonnet, D., Briole, P. and A. Arnaud (1995): "Deflation of Mount Etna monitored by spaceborne radar interferometry." *Nature*, 375(June), pp. 567-570.
- Massonnet, D. and T. Rabaute (1993): "Radar interferometry: limits and potential." *IEEE Transactions on Geoscience and Remote Sensing*, 31(2), pp. 455-464.
- Monti Guarnieri, A. and C. Prati (1996): "ScanSAR focusing and interferometry." *IEEE Transactions on Geoscience and Remote Sensing*, 34(4), pp. 1029-1038.
- Monti Guarnieri, A., Prati, C. and F. Rocca (1994): "Interferometry with ScanSAR." *EARS&L Newsletter*, Dec.(20).
- Moore, R. K., Claassen, J. P. and Y. H. Lin (1981): "Scanning spaceborne synthetic aperture radar with integrated radiometer." *IEEE Transactions on Aerospace and Electronic Systems*, 17(3), pp. 410-420.
- Moreira, A., Mittermayer, J. and R. Scheiber (1996): "Extended Chirp Scaling algorithm for air- and spaceborne SAR data processing in stripmap and ScanSAR image modes." *IEEE Transactions on Geoscience and Remote Sensing*, 34(5), pp. 1123-1136.
- Prati, C. and F. Rocca (1990): "Limits to the resolution of elevation maps from stereo SAR images." *International Journal of Remote Sensing*, 11(12), pp. 2215-2235.
- Rodriguez, E. and J. M. Martin (1992): "Theory and design of interferometric synthetic aperture radars." *IEEE Proceedings-F*, 139(2), pp. 147-159.
- Roth, A., Knöpfle, W., Hubig, M. and N. Adam (1998): "Operational interferometric SAR products." *International Geoscience and Remote Sensing Symposium IGARSS'98*, pp. 324-326.
- Tomiyasu, K. (1981): "Conceptual performance of a satellite borne, wide swath synthetic aperture radar." *IEEE Transactions on Geoscience and Remote Sensing*, GE-19(2), pp. 108-116.
- Zebker, H. A. and R. M. Goldstein (1986): "Topographic mapping from interferometric synthetic aperture radar observations." *Journal of Geophysical Research*, 91(B 5), pp. 4993-4999.
- Zebker, H. A. and J. Villasenor (1992): "Decorrelation in interferometric radar echoes." *IEEE Transactions on Geoscience and Remote Sensing*, 30(5), pp. 950-959.